

Study on Dynamic Hysteretic Nonlinear Property in time-domain of Site Soil from Site strong Response During March 11, 2011 Japan M9.0 Earthquake



CHEN Xueliang, GAO Mengtan, LI Tiefei & YAN Zhaolun

Division of Engineering Earthquake and City Disaster Reduction, Institute of Geophysics, China Earthquake Administration, Beijing, China.

SUMMARY:

The analysis of hysteretic nonlinear property in time domain of site soils are rare at home and abroad for the complexity of soil dynamic nonlinear constituted relations, low efficiency of implicit integral formula, and low performance of optimized method. In view of these questions, this paper using soil dynamic double- parabola constitute model, which can consider the soil test damping ratio and can character main characteristic of soil's hysteretic constituted relationship, associating with the highly effective explicit integral method with the high accuracy computation acceleration response, basing on 201103111446 M9.0 and its strong foreshock 201103091145 M7.2. The hysteretic nonlinear characteristic in time domain of the clay and the granite at FKSH19 borehole array are analyzed. The results indicated that, the modulus and the damping ratio of clay and the granite are consistent with the lab test results of Seed-Idriss. It is different that viscous damping effects in the strong earthquake and weak ground motion. The mechanism and the history of hysteretic nonlinear constituted relationship under seismic strong motion are reproduced. The results reveal the permanent displacement mechanism. Simultaneously, velocity history and displacement history of ground strong motion are forecasted and estimated.

Keywords: Hysteretic nonlinear property, viscous damping, strain-dependent, shear modulus ratio, hysteretic damping

1. INTRODUCTION

On March 11, 2011 at 2:46 PM (local time), the Northeast coast of Japan occurred Ms9.0 great earthquake, which is abbreviated as 201103111446 M9.0 Earthquake, resulting in approximately 20m of vertical slip and causing a devastating tsunami, then, the Ms9.0 great earthquake and tsunami caused Japan serious nuclear accident. These resulted in approximately 15,000 fatalities, approximately 12,000 missing, displaced 160,000, and caused an estimated \$200- \$300 (USD) billion in losses(SEAW, 2011). The ground motion records indicate very strong ground shaking ($>1.0g$) with long duration (>3.0 minutes). The earthquake caused serious geological disasters and geotechnical disasters, such as, landslides and rock falls that occurred in areas of past instability, liquefaction that occurred in areas with loose to medium-dense, saturated sand and silt, especially reclaimed land (e.g., Urayasu City), liquefaction damage was extensive, even at sites over 150 km from the fault rupture, and ground and structure settlement were often found (SEAW, 2011). During this great earthquake, 1224 stations in Japan KiK-net and K-NET seismic network (from KiK-net & K-NET html) obtained high-quality strong motion records.

201103111446 M9.0 Earthquake have a number of strong foreshocks and aftershocks, almost at the same location, M7.2 Earthquake on March 09, 2011 at 11:45 AM (local time), which is called 201103091145 M7.2 Earthquake, is very important for its large magnitude before the M9.0 Earthquake. Borehole array FKSH19 station record two seismic waveforms of these earthquakes very well. The surface Peak Ground Acceleration (PGA) of 201103111446 M9.0 Earthquake is 692gal, while PGA of 201103091145 M7.2 Earthquake is 24.8gal, the difference of the strong motion strength is obvious. It is very important for the study of nonlinear dynamic characteristics of soil.

Borehole array FKSH19 has clear soil profile, which is simple typical site. According to Japan KiK-net and K-NET seismic network, in addition to high-quality strong motion records, we can get

geological material, soil types, thickness, the small strain shear velocity, P velocity, geological time, elevation and the depth etc. But, strain-dependent shear modulus ratio $G_d/G_{\max} \sim \gamma$ and damping ratio $\lambda \sim \gamma$, which are very important nonlinear dynamic characteristics parameters of soil, are unknown. How do we get the dynamic nonlinear parameters of the FKSH19 site soil?

On the other hand, under the ground motions action, the damping of the soil is divided into two types, one is the hysteretic damping, and the other is viscous damping. As we all known, strong ground motion and weak ground motions, soil nonlinear hysteretic constitutive relationship is different, that is, the hysteretic damping is different. However, both cases, whether the viscous damping effect have changed or not? At present, relevant reports have not been seen yet, we tried to explore this.

The nonlinear method of site response in time domain has been more and more attention for it can actually reflect the primary characteristics of site response, such as “along with the seismic motion increases, the nonlinear response strengthen, the response amplitude decrease, the predominant period moves to the long period range” etc. However, the site response results of equivalent linearization method with the questions of “false resonating”, when it processes “the strong motion input”, “the soft layer” cases, are not consistent with the observation records.

Based on soil experiment achievements of strain-dependent shear modulus and damping ratio according to skeleton curve equation, many kinds of soil dynamic nonlinear constitutive models, such as the General Masing rule, Pyke method(Pyke, 1979), Hardin-Drnevich(Hardin and Drnevich, 1972a, 1972b) hyperbolic curve model, Ramberg-Osgood(R-O) model(Ramberg and Osgood, 1943), Martin-Davidenkova(M-D) model(Martin, 1975), Iwan model (Iwan, 1967)and Revised Iwan model (Zheng D.T. & Wang H.C., 1983) and so on, have been established. Considering the shape of reverse load curves or unload curves sometimes does not have specific changes in the law, one soil dynamic double-parabola constitutive model with adjustable constitutive curves shape (A_d is Adjustment factor), was proposed by Chen X.L. et al. (2008).

Explicit algorithm in time-domain are widely applied in many fields, which are the non-linear dynamic response analysis of a large-scale complex system, the digital control of pseudo-dynamic experiment, real-time simulation analysis of computer, etc. for its small computation with high computational efficiency and so on advantages. In this study, Newmark “New” Explicit Step-by-step Integration Formulas (Chen X.L. et al., 2009) with calculating displacement, velocity and acceleration response simultaneously, are used.

2. BOREHOLE ARRAY FKSH19 STATION AND STRONG MOTION RECORDS

Japan KiK-net and K-NET seismic network provides some information and strong motion records of the borehole array FKSH19 (37.4672N, 140.7261E) station at the site of Miyakoji village, Tamura county in Fukushima Prefecture. The location of borehole array FKSH19 and the two earthquakes, which are 201103111446 M9.0 and 201103091145 M7.2, are given in Figure 1. The depth of hypocenter of 201103111446 M9.0 Earthquake is about 24km, the epicentre is (38.0N 142.9E), the distance from the station to the epicentre is 249 km, the surface seismic motion PGA is 692gal, as mentioned earlier. Similarly, the depth of hypocenter of 201103091145 M7.2 Earthquake is 8km, the epicentre is (38.328N 143.278E), the distance from the station to epicentre is 299 km, the surface seismic motion PGA is 24.8gal. By calculating, back - azimuths of 201103111446 M9.0 Earthquake and 201103091145 M7.2 Earthquake are respectively 76.2°and 71.4°.

According to Japan KiK-net and K-NET seismic network, we get a cross section of FKSH19 borehole, as shown in Figure 2. In this borehole array site, three-component broadband seismographs at both the surface (GL-0m) and the bedrock (GL-103m) are established. Two high-quality seismic 201103111446 M9.0 and 201103091145 M7.2 are recorded. The researchers(or the staff) in Japan KiK-net and K-NET seismic network said, in addition to the information of the net-site, they do not

have any other information of borehole soil layer, including strain-dependent shear modulus ratio $G_d/G_{max} \sim \gamma$ and damping ratio $\lambda \sim \gamma$, viscous damping of the borehole soil in the small strain range, etc.

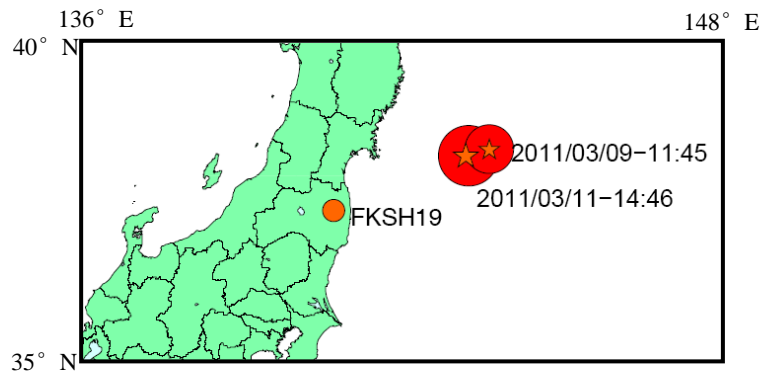


Figure 1. The location of borehole array FKSH19 and the two earthquakes

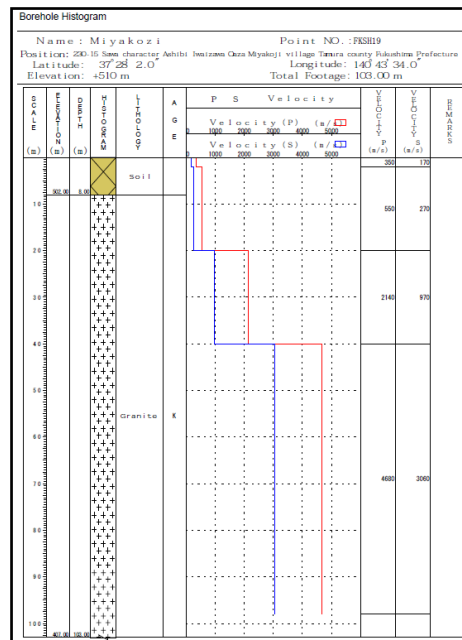


Figure 2. Soil and rock condition of FKSH19 site

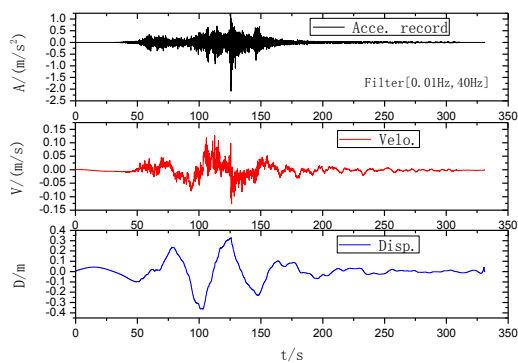


Figure 3. The time history of acceleration, velocity, displacement of 201103111446 M9.0 Earthquake at bedrock

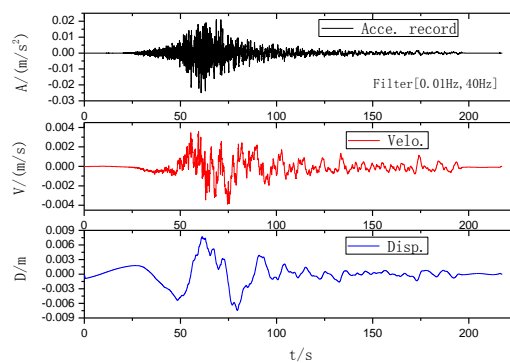


Figure 4. The time history of acceleration, velocity, displacement of 201103091145 M7.2 Earthquake at bedrock

Instrument record is voltage signal, through the transformation, the original acceleration signal are obtained, using China conventional treatment procedures, which include eliminated the background of white noise, eliminated the zero-line drift, calculus, Butterworth filter(20 order) Filtering, etc, the time history of three-component(EW, NS, UD) of acceleration, velocity, displacement are obtained. According to back-azimuth of each earthquake and FKSH19 station, SH-wave fields are isolated from the records (EW, NS component) of the bedrock and the surface. The time history of “SH” acceleration, “SH” velocity, “SH” displacement of 201103111446 M9.0 Earthquake and 201103091145 M7.2 Earthquake, are shown in Figure 3 and Figure 4 respectively. In fact, only the SH acceleration wave comes from the EW and NS component of the records, the SH velocity wave and SH displacement wave is equivalent to the integral first or the integral twice of the SH acceleration wave. They are gotten indirectly.

In this study, the only SH-wave fields are analyzed. At the same time, at the bottom (the bedrock) of FKSH19 station, the boundary condition is artificial boundary condition, which is regarded as Multi-Transmitting Formula (abbreviated as MTF) condition (Liao Z. P., 1984, 2002). This boundary condition make the reflected wave (outside waves) are freely transmit. Simultaneously, SH-wave at the bedrock are assumed vertical incidence.

3. SOIL CONSTITUTIVE MODEL AND NUMERICAL SIMULATION METHOD

3.1. Soil dynamic double-parabola constitutive model(CHEN Xue-liang, JIN Xing et al, 2008)

Based on the basic characteristic curves $G/G_{\max} - \gamma$ and $\lambda - \gamma$ revealed by the results of the soil dynamic tests, the rules of adjustable double-parabola constitutive curves of reverse unload after load process or reverse load after unload process in irregular load history are established by Chen X.L., Jin X. et al.(2008). The model can be a good simulation of test damping ratio in the irregular load history.

The equation of soil dynamic double-parabola constitutive model is,

$$\tau(\gamma) = \begin{cases} \frac{G_{\max}\gamma}{1+|\gamma|/\gamma_r} & |\gamma| \geq \gamma_M \\ (1-A_d)\tau_-^A + A_d\tau_-^B & d\gamma < 0 \\ (1-A_d)\tau_+^A + A_d\tau_+^B & d\gamma \geq 0 \end{cases} \quad |\gamma| < \gamma_M \quad (1)$$

Where, supposed $A_d = 0.8$. $\tau_-^B = 2\tau_0 - \frac{-b_2 + \sqrt{b_2^2 - 4a_2(c_2 - 2\gamma_0 + \gamma)}}{2a_2}$;

$\tau_-^A = 2\tau_0 - a_1(2\gamma_0 - \gamma)^2 - b_1(2\gamma_0 - \gamma) - c_1$; $\tau_+^B = \frac{-b_2 + \sqrt{b_2^2 - 4a_2(c_2 - \gamma)}}{2a_2}$; $\tau_+^A = a_1\gamma^2 + b_1\gamma + c_1$;

$a_1 = -1.5\pi\lambda_T(\gamma_0)\frac{\tau_M - \tau_C}{(\gamma_M - \gamma_C)^2}$; $b_1 = \frac{(\tau_M - \tau_C)}{(\gamma_M - \gamma_C)}\left(1 + 1.5\pi\lambda_T(\gamma_0)\frac{\gamma_M + \gamma_C}{\gamma_M - \gamma_C}\right)$;

$c_1 = \frac{\gamma_M\tau_C - \gamma_C\tau_M}{\gamma_M - \gamma_C} - 1.5\pi\lambda_T(\gamma_0)\frac{\gamma_M\gamma_C(\tau_M - \tau_C)}{(\gamma_M - \gamma_C)^2}$; $a_2 = 1.5\pi\lambda_T(\gamma_0)\frac{\gamma_M - \gamma_C}{(\tau_M - \tau_C)^2}$;

$b_2 = \frac{\gamma_M - \gamma_C}{\tau_M - \tau_C}\left(1 - 1.5\pi\lambda_T(\gamma_0)\frac{\tau_M + \tau_C}{\tau_M - \tau_C}\right)$; $c_2 = \gamma_M - a_2\tau_M^2 - b_2\tau_M$.

γ_c and τ_c was the corresponding strain and the stress of “the inflexion point” in recently load (or unloading) process. (τ_M, γ_M) is the point of the biggest stress and the biggest strain in history, the biggest stress and the biggest strain are always positive. $\lambda_r(\gamma_0)$ is experimental damping ratio. A_d is adjustment factor, which means the proportion in total constitutive characteristics. That is, the characteristics of reverse unload curves or reverse load curves change more acutely at first and then flatly, its proportion. In this paper, A_d is 0.8.

3.2 Wave propagation finite element method

Ideas of decoupled near-field wave propagation numerical simulation, which are the combination of Multi-Transmitting Formula (abbreviated as MTF) and the concentrated mass explicit finite element method, are proposed by Liao Z. P. and his collaborators (Liao Z. P., 1984, 2002; Li X. J., et al., 1992). This is often referred to as the “Wave Propagation Finite Element Method”. The “inner nodes” calculations of this method need a explicit numerical integration formulas in time-domain, Newmark “new” explicit step-by-step integration formulas ($\gamma = 1/2, \beta = 1/6$, the third format), which proposed by Chen X.L., et al.(2009), are used in this study. The method is decoupled in space, is explicit in time, compared to other implicit methods, computer memory is small, computation efficient is high. Equation expression of the third format ($\gamma = 1/2, \beta = 1/6$) are,

$$\begin{aligned} \{u(t+\Delta t)\} &= \frac{\Delta t^2}{2} [M]^{-1} \{F(t)\} + \left([I] - \frac{\Delta t^2}{2} [M]^{-1} [K] \right) \{u(t)\} + \left(\Delta t [I] - \frac{\Delta t^2}{2} [M]^{-1} [C] \right) \{\dot{u}(t)\} \\ \{\dot{u}(t+\Delta t)\} &= \frac{1}{2} \Delta t [M]^{-1} (\{F(t+\Delta t)\} + \{F(t)\}) - \left[\frac{1}{2} \Delta t [M]^{-1} [K] + \frac{3}{2} [M]^{-1} [C] \right] \{u(t+\Delta t)\} \\ &\quad + \left(\frac{3}{2} [M]^{-1} [C] - \frac{1}{2} \Delta t [M]^{-1} [K] \right) \{u(t)\} + \left([I] + \frac{1}{2} \Delta t [M]^{-1} [C] \right) \{\dot{u}(t)\} \\ &\quad + \frac{1}{4} \Delta t^2 [M]^{-1} [C] \{\ddot{u}(t)\} \\ \{\ddot{u}(t+\Delta t)\} &= [M]^{-1} \{F(t+\Delta t)\} - [M]^{-1} [C] \{\dot{u}(t+\Delta t)\} - [M]^{-1} [K] \{u(t+\Delta t)\} \end{aligned} \quad (2)$$

Where, $[M], [C], [K]$ are respectively mass matrix, damping matrix and stiffness matrix of the system. $\{u(t+\Delta t)\}, \{\dot{u}(t+\Delta t)\}, \{\ddot{u}(t+\Delta t)\}$ and $\{F(t+\Delta t)\}$ are the node displacement, velocity, acceleration response and the external load at the $t+\Delta t$ moment, respectively. Viscous damping matrix $[C]$ are assumed to be Rayleigh damping, $[C] = \alpha [M] + \beta [K]$, α, β are damping coefficients. $[K]$ are determined by nonlinear constitutive relations in §3.1.

4. SUPPLEMENT THE MODEL PARAMETERS & NUMERICAL SIMULATION ANALYSIS

FKSH19 site model are listed in Table 1. FKSH19 site model has no density ρ and viscous Damping ratio ξ , according to soil type, lithology, etc., we added these two types of parameters, which are listed in Table 1. Viscous damping matrix $[C]$ are assumed two types. First, $[C] = \alpha [M] = 2\xi\omega'_0 [M]$, ω'_0 is experience the circular frequency, experience value is 90rad/s in this paper. Second, $[C] = \beta [K] = \frac{2\xi}{\omega'_0} [M]$, parameters are the same. The parameters of hysteretic constitutive curve and

hysteretic damping, which include strain-dependent shear modulus ratio and damping ratio of miscellaneous fill (clay) and granite (rock), are introduced. Strain-dependent shear modulus ratio of

miscellaneous fill (clay) uses Seed & Sun(1989)'s result, and strain-dependent damping ratio of miscellaneous fill (clay) uses Idriss(1990)'s result. While strain-dependent shear modulus ratio and damping ratio of granite (rock) derived from the rock result of program SHAKE91, In the large strain range, parameters were added. Figure 5 and Figure 6 give the nonlinear parameters of miscellaneous fill (clay) and granite (rock) respectively. In the end, the seismic hysteretic nonlinear response of site in two-type viscous damping form is calculated respectively.

Table 1. 21-sub-soil-layer model of FKSH19 site

| No. | Soil description | Soil type No. (Adjacent to the layer (below)) | Layer deepness(m) (Origin in the bedrock; Upward is positive) | Shear wave velocity V_s (m/s) | Density ρ (kg/m ³) | Viscous Damping ratio ξ |
|-----|--------------------|---|---|---------------------------------|-------------------------------------|-----------------------------|
| 1 | Granite | 2 | 0.0 | 3060 | 2300 | 0.015 |
| 2 | Granite | 2 | 8.0 | 3060 | 2300 | 0.015 |
| 3 | Granite | 2 | 16.0 | 3060 | 2300 | 0.015 |
| 4 | Granite | 2 | 24.0 | 3060 | 2300 | 0.015 |
| 5 | Granite | 2 | 32.0 | 3060 | 2300 | 0.015 |
| 6 | Granite | 2 | 40.0 | 3060 | 2300 | 0.015 |
| 7 | Granite | 2 | 48.0 | 3060 | 2300 | 0.015 |
| 8 | Granite | 2 | 56.0 | 3060 | 2300 | 0.015 |
| 9 | Granite | 2 | 63.0 | 3060 | 2300 | 0.015 |
| 10 | Granite | 2 | 68.0 | 970 | 2200 | 0.018 |
| 11 | Granite | 2 | 73.0 | 970 | 2200 | 0.018 |
| 12 | Granite | 2 | 78.0 | 970 | 2200 | 0.018 |
| 13 | Granite | 2 | 83.0 | 970 | 2200 | 0.018 |
| 14 | Granite | 2 | 86.0 | 270 | 2100 | 0.020 |
| 15 | Granite | 2 | 89.0 | 270 | 2100 | 0.020 |
| 16 | Granite | 2 | 92.0 | 270 | 2100 | 0.020 |
| 17 | Granite | 2 | 95.0 | 270 | 2100 | 0.020 |
| 18 | clay | 1 | 97.0 | 270 | 1900 | 0.025 |
| 19 | clay | 1 | 99.0 | 270 | 1900 | 0.025 |
| 20 | clay | 1 | 101.0 | 270 | 1900 | 0.025 |
| 21 | Miscellaneous fill | 1 | 103.0 | 170 | 1850 | 0.028 |

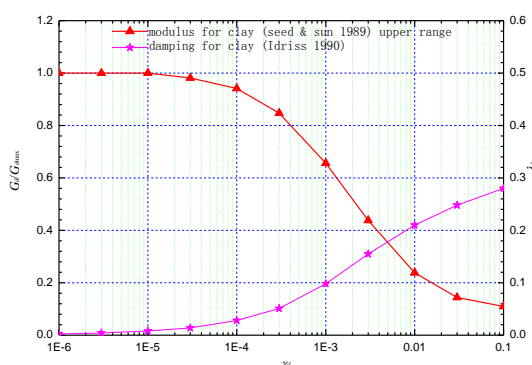


Figure 5. Strain-dependent shear modulus ratio and damping ratio of miscellaneous fill (clay)

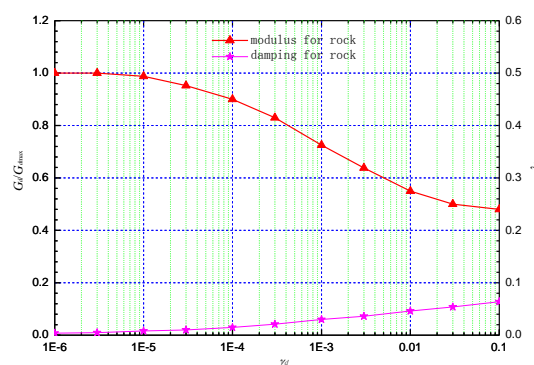


Figure 6. Strain-dependent shear modulus ratio and damping ratio of granite (rock)

Comparison of the calculation acceleration, velocity and displacement and record results of 201103111446 M9.0 Earthquake, respectively, are shown in Figure 7, these of 201103091145 M7.2 Earthquake are shown in Figure 11. Comparison of response spectrum and its ratio of record acceleration at surface and bedrock of 201103111446 M9.0 Earthquake, respectively, are given in

Figure 8, Fourier spectrum ratio case of 201103111446 M9.0 Earthquake are given in Figure 9. Similarly, comparison of response spectrum and its ratio of record acceleration at surface and bedrock of 201103091145 M7.2 Earthquake, respectively, are given in Figure 12, Fourier spectrum ratio case of 201103091145 M7.2 Earthquake are given in Figure 13. In Figure 10, comparison of nonlinear constitutive relations at 21th, 18th, 14th, 10th sub-layer of 201103111446 M9.0 Earthquake, respectively.

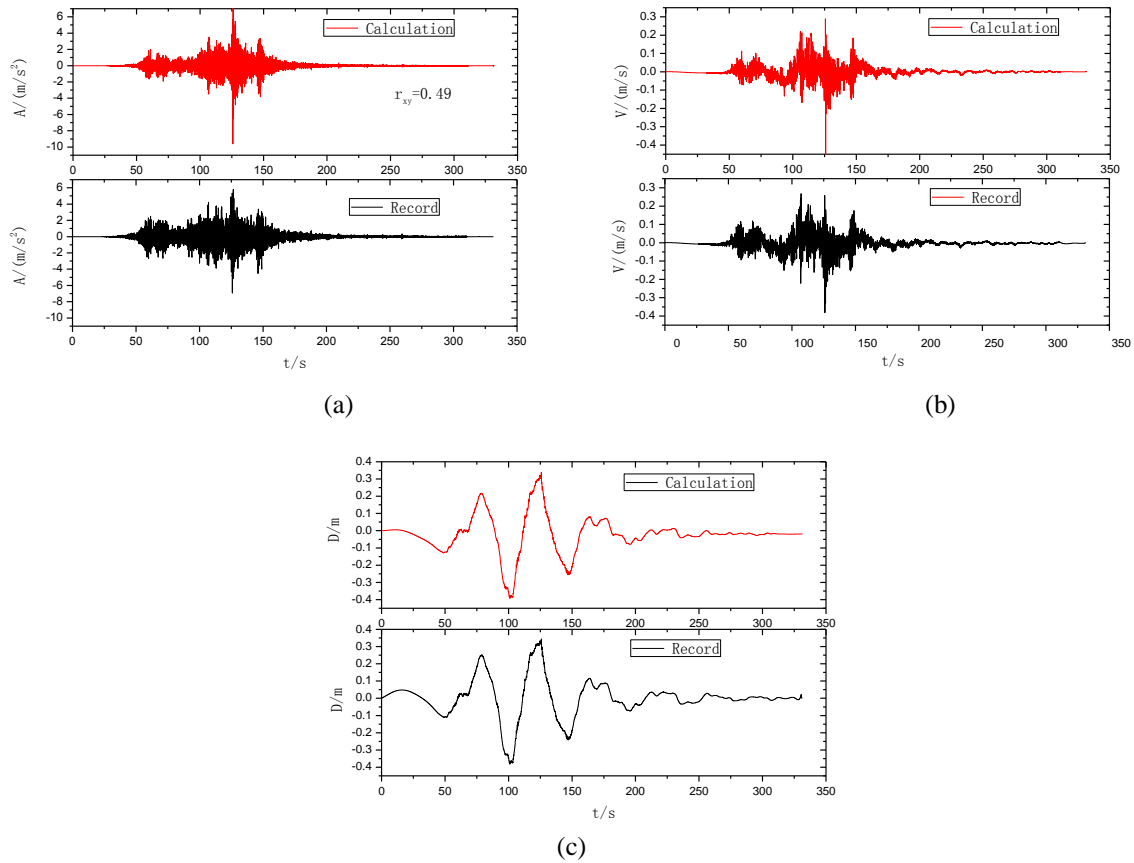


Figure 7. Comparison of the calculation acceleration, velocity and displacement and record results of 201103111446 M9.0 Earthquake, respectively

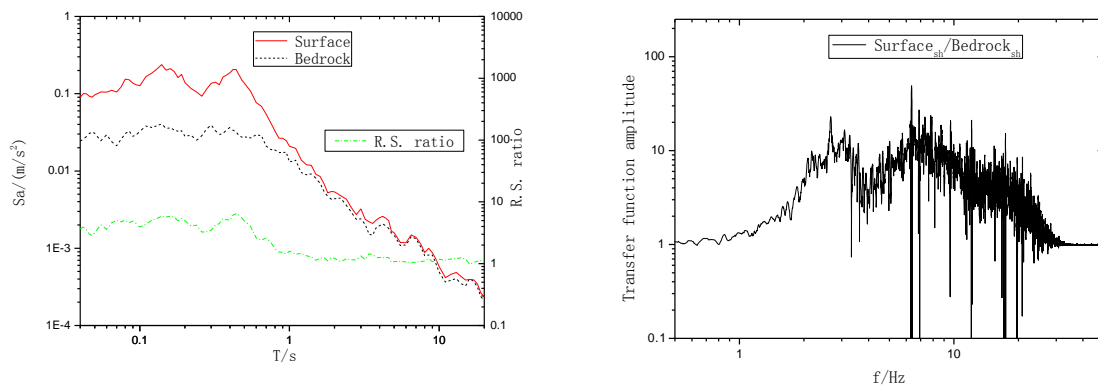


Figure 8. Comparison of response spectrum and its ratio of record acceleration at surface and bedrock of 201103111446 M9.0 Earthquake, respectively

Figure 9. Comparison of Fourier spectrum ratio of record acceleration at surface and bedrock of 201103111446 M9.0 Earthquake, respectively

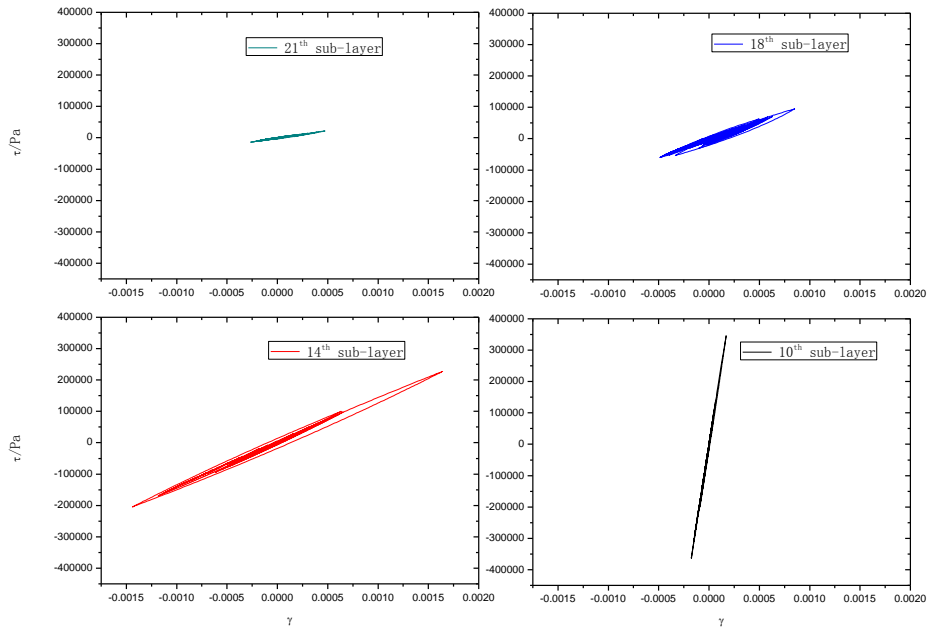


Figure 10. Comparison of nonlinear constitutive relations at 21th, 18th, 14th, 10th sub-layer of 201103111446 M9.0 Earthquake, respectively

For Fourier spectrum ratio's smoothing, Savitzky-Golay Method with 30 points of window and polynomial order 2, are used in Figure 10 and Figure 13.

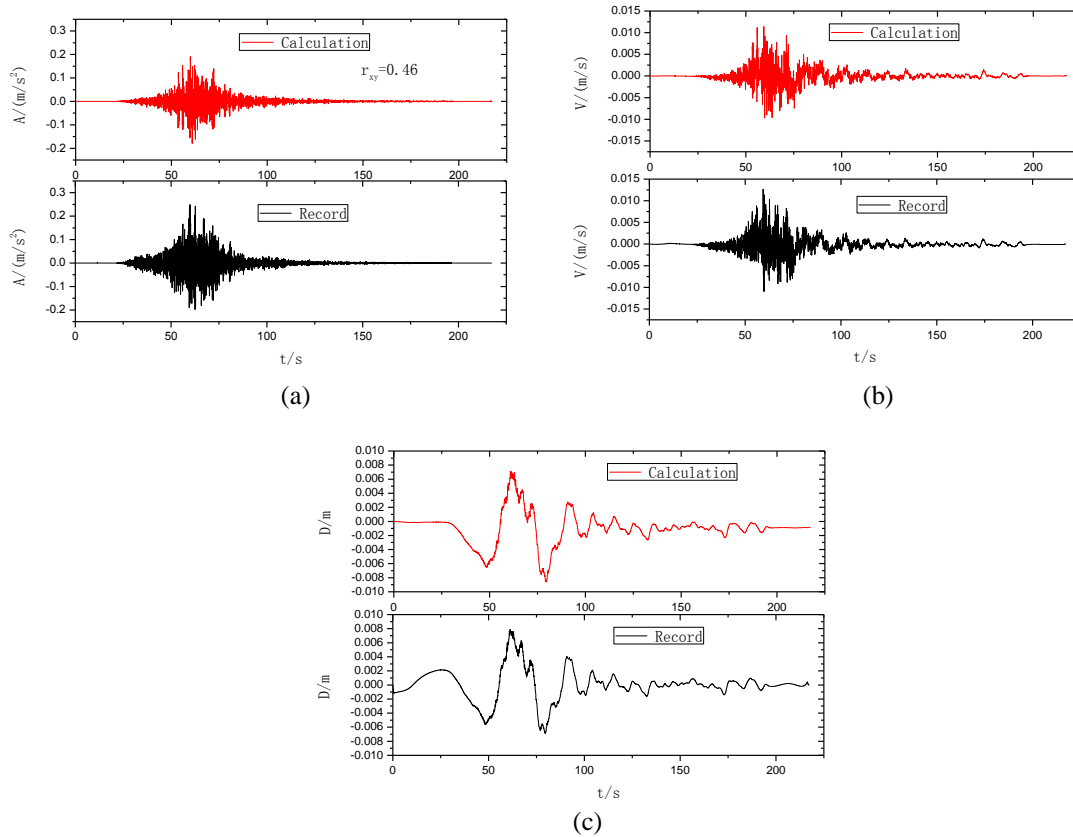


Figure 11. Comparison of the calculation acceleration, velocity and displacement and record results of 201103091145 M7.2 Earthquake, respectively

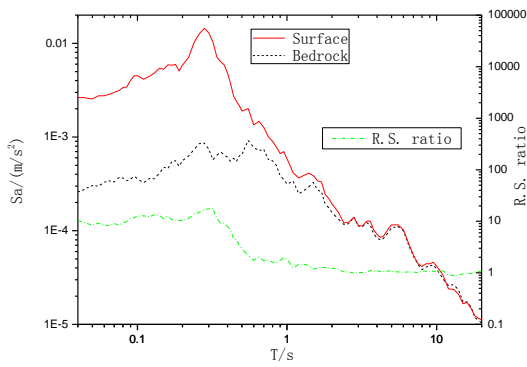


Figure 12. Comparison of response spectrum and its ratio of record acceleration at surface and bedrock of 201103091145 M7.2 Earthquake, respectively

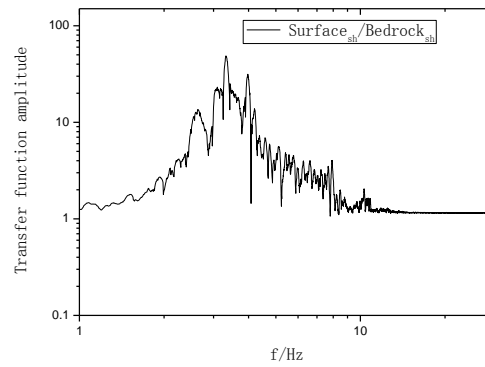


Figure 13. Comparison of Fourier spectrum ratio of record acceleration at surface and bedrock of 201103091145 M7.2 Earthquake, respectively

From Figure 7 and Figure 11, the results indicated: using pervious given strain-dependent shear modulus ratio and damping ratio of miscellaneous fill (clay) and granite(rock), density and viscous damping ratio, the calculation nonlinear acceleration response, velocity response and displacement response are quite consistent with the record results of 201103111446 M9.0 Earthquake and 201103091145 M7.2 Earthquake, respectively.

From Figure 8,9 and Figure 12,13, we can found, the prominent period of FKSH19 in 201103091145 M7.2 Earthquake are about 0.3s, the frequency is about 3.3Hz, the amplification factor is about 20, However, the prominent period of FKSH19 in 201103111446 M9.0 Earthquake are about 0.45s, the frequency is about 2.2Hz, the amplification factor is about 45. These reflect significantly the nonlinear characteristics of the site.

Nonlinear constitutive relations of 4 sublayers of FKSH19 site in 201103111446 M9.0 Earthquake, that reflect the nonlinear constitutive history of soil layer's vibration during the strong motion of 201103111446 M9.0 Earthquake. By the calculation displacement in Figure 7 and Figure 11, 19.3mm and 1 mm permanent displacement in 201103111446 M9.0 Earthquake and 201103091145 M7.2 Earthquake, are calculated respectively.

Calculation process of analysis, we found that, the same hysteretic constitutive rules, in 201103111446 M9.0 Earthquake, $\alpha[M]$ -type viscous damping is better than $\beta[K]$ -type viscous damping for agreement with the record result. But, in 201103091145 M7.2 Earthquake, on the contrary, $\beta[K]$ -type viscous damping is better than $\alpha[M]$ -type viscous damping for agreement with the record result.

5. DISCUSSION AND CONCLUSION

1.Viscous damping of FKSH19 site is $\alpha[M]$ -type in 201103111446 M9.0 Earthquake, on the contrary, it is $\beta[K]$ -type in 201103091145 M7.2 Earthquake. Strong ground motion can cause that, along with the seismic motion increases, the nonlinear response strengthen, the response amplitude decrease, the predominant period moves to the long period range.

2. Nonlinear soil property on shearing strain can be calculated when large-scale strain occurred during a strong ground motion. Seed & Sun(1989)'s strain-dependent shear modulus ratio, and Idriss(1990)'s strain-dependent damping ratio test result for miscellaneous fill (clay), the rock test result of program SHAKE91 for the granite(rock), all agree with nonlinear dynamic characteristics of FKSH19 site soil.

3. Soil dynamic hysteretic nonlinear response method of site in time domain can rebuild soil dynamic constitutive history of hysteretic nonlinear site in time domain, predict and evaluate site velocity time history, and reveal site displacement time history and mechanism of static displacement.

ACKNOWLEDGEMENT

This work was financially supported by the China National Special Fund for Earthquake Scientific Research in Public Interest (grants 2010008001); the Scientific Research Institutes' Basic Research and Development Operations Special Fund of the Institute of Geophysics, China Earthquake Administration (grant DQJB11C15, DQJB129902); and the National Natural Science Foundation of China (grants 90915012 and 50808162).

REFERENCES

- SEAW Reconnaissance Team(2011). 2011 great east Japan (tohoku) earthquake & tsunami. SEAW Japan EQ. Report.
- Masing. (1926).G. Eigenspannungen und verfestigung beim Messing. *Proceedings of the 2nd International Congress on Applied Mechanics, Zurich*.
- Pyke, R. (1979). Nonlinear Soil Models for Irregular Cyclic Loadings. *Journal of the Geotechnical Engineering Division, ASCE*, **105:6**, 715-725.
- Hardin, B. O., Drnevich, V. P.(1972a). Shear modulus and damping in soil: measurement and parameter effects. *Journal of the Soil mechanics and Foundation Engineering Division, ASCE*, **98:6**, 603-624.
- Hardin, B. O., Drnevich, V. P.(1972b). Shear modulus and damping in soil: design equations and curves. *Journal of the Soil mechanics and Foundation Engineering Division, ASCE*, **98:7**, 667-692.
- Ramberg, W. and Osgood, W.(1943). Description of Stress Strain Curves by Three Parameters. Technical Note No. 902, National Advisory Committee for Aeronautics, Washington, DC.
- Martin, P. P.(1975). Nonlinear Method for Dynamic Analysis of Ground Response [Ph. D. Thesis][D]. University of California, Berkeley, June.
- Iwan, W. D. (1967). On a Class of Models for the Yielding Behavior of Continuous and Composite Systems. *Journal of Applied Mechanics*, **34:3**, 612-617.
- Zheng D.T., Wang H.C.(1983). Nonlinear stress-strain models of soils under cyclic loadings. *Chinese Journal of Geotechnical Engineering*, **5:1**, 65-75.
- Liao, Z.P.(1984). A finite element method for near-field wave motion in heterogeneous materials. *Earthquake Engineering and Engineering Vibration*, **4:2**, 1-14.
- Liao, Z.P.(2002). Engineering Introduction to Wave Theory [M]. Beijing: Science Press, 2002.
- Li, X.J., Liao, Z.P., Du, X.L.(1992). An explicit finite difference method for viscoelastic dynamic problem. *Earthquake Engineering and Engineering Vibration*, **12:4**, 74-80.
- Chen X.L., Gao M.T., Tao X.X.(2009).Newmark "New" Explicit Step-by-step Integration Formulas. *Journal of Harbin Institute of Technology (New Series)*, **16(Sup.1)**, 84-91.
- Chen X.L., Jin X., Tao X.X. et al.(2008). One soil dynamic double-parabola constitutive model considering the effect of soil test damping, *Rock and Soil Mechanics*, **29:8**, 2102-2110.
- K-NET, KiK-net. http://www.kik.bosai.go.jp/kik/index_en.shtml